Elovanoids counteract oligomeric β-amyloid-induced gene expression and protect photoreceptors

Khanh V. Do[a], Marie-Audrey I. Kautzmann[a], Bokkyoo Jun[a], William C. Gordon[a], Robert Nshimiyimana[b], Rong Yang[b], Nicos A. Petasis[b], and Nicolas G. Bazan[a,1]

[a]Neuroscience Center of Excellence, School of Medicine, Louisiana State University Health New Orleans, New Orleans, LA 70112; and [b]Department of Chemistry and Loker Hydrocarbon Research Institute, University of Southern California, Los Angeles, CA 90089-1661

Edited by Solomon H. Snyder, Johns Hopkins University School of Medicine, Baltimore, MD, and approved October 1, 2019 (received for review July 26, 2019)

The onset of neurodegenerative diseases activates inflammation that leads to progressive neuronal cell death and impairments in cognition (Alzheimer's disease) and sight (age-related macular degeneration [AMD]). How neuroinflammation can be counteracted is not known. In AMD, amyloid β-peptide (Aβ) accumulates in subretinal drusen. In the 5xFAD retina, we found early functional deficiencies (ERG) without photoreceptor cell (PRC) death and identified early insufficiency in biosynthetic pathways of prohomeostatic/neuroprotective mediators neuroprotectin D1 (NPD1) and elovanoids (ELVs). To mimic an inflammatory milieu in wild-type mouse, we triggered retinal pigment epithelium (RPE) damage/PRC death by subretinally injected oligomeric β-amyloid (OAβ) and observed that ELVs administration counteracted their effects, protecting these cells. In addition, ELVs prevented OAβ-induced changes in gene expression engaged in senescence, inflammation, autophagy, extracellular matrix remodeling, and AMD. Moreover, as OAβ targets the RPE, we used primary human RPE cell cultures and demonstrated that OAβ caused cell damage, while ELVs protected and restored gene expression as in mouse. Our data show OAβ activates senescence as reflected by enhanced expression of $p16^{INK4a}$, MMP1, p53, p21, p27, and Il-6, and of senescence-associated phenotype secretome, followed by RPE and PRC demise, and that ELVs 32 and 34 blunt these events and elicit protection. In addition, ELVs counteracted OAβ-induced expression of genes engaged in AMD, autophagy, and extracellular matrix remodeling. Overall, our data uncovered that ELVs downplay OAβ-senescence program induction and inflammatory transcriptional events and protect RPE cells and PRC, and therefore have potential as a possible therapeutic avenue for AMD.

retinal pigment epithelial cells | age-related macular degeneration | senescence gene program | p16 | SASP

The onset of the neuroinflammatory response encompasses synthesis of endogenous mediators aiming to counteract brain and/or retina damage. Neuroprotectin D1 (NPD1), a docosanoid derived from an omega-3 essential fatty acid, is neuroprotective by arresting inflammation initiation, and thus sustaining photoreceptor cell (PRC) integrity (1), and is deficient in the hippocampus CA1 area of early Alzheimer's disease (AD) (2). Aβ accumulates in AD. In the 5xFAD retina, Aβ also accumulates, and although Aβ in AMD sets in motion homeostasis disturbances that include inflammation and contribute to PRC death (3, 4), it is not known how to limit Aβ-mediated cell damage. In PRCs, very long chain polyunsaturated fatty acids (VLC-PUFAs, C > 28) are synthesized by ELOVL4 (elongation of very long chain fatty acid-4) (5, 6) and are necessary for rhodopsin function (7). Mutations on the ELOVL4 gene (5) cause Stargardt macular dystrophy type 3 with central vision loss. Recessive ELOVL4 mutations cause seizures, mental retardation, and spastic quadriplegia, suggesting the importance of VLC-PUFAs in brain development and physiology, as well (8). Once VLC-PUFAs are incorporated into specific phosphatidylcholine molecular species (PCs) of the photoreceptor cells outer segments, they arrive to the retinal pigment epithelium (RPE) after daily PRC disk shedding and phagocytosis. Elovanoids (ELVs) with 32 and 34C are enzymatically synthesized in RPE cells from PC-released VLC-PUFAs by a phospholipase A1 (9, 10). These novel lipid mediators have the ability to protect RPE cells from uncompensated oxidative stress by up-regulating prohomeostatic and prosurvival protein abundance with attenuation of apoptosis in photoreceptor cells (9, 10), as well as in neurons (10, 11).

Aβ42 is a component of drusen in AMD, and of senile plaques of AD (12, 13). In AMD, Aβ contributes to inflammation, perturbed RPE morphology and function, and PRC integrity (14, 15). The 5xFAD transgenic mouse carries mutations associated with early-onset familial AD, and although it displays several unspecific changes, it shows PRC degeneration (16, 17). We first investigated the 5xFAD retinal phospholipid profile seeking to understand the availability of precursors of lipid mediators preceding the expression of PRC degeneration in the 5xFAD mice. Next, we studied the consequences of subretinal administration of oligomeric Aβ (OAβ), one of the most cytotoxic forms of Aβ, in wild-type (WT) mice on RPE and PRC, as well as on the expression of genes involved in senescence, autophagy, AMD, extracellular matrix (ECM) remodeling, and apoptosis. Also, we exposed human RPE cells in culture to OAβ and assessed similar endpoints. Finally, we evaluated whether or not ELVs modify OAβ-induced gene expression, including the senescence program and

Significance

This study uncovers biosynthetic pathway insufficiencies of prohomeostatic/neuroprotective mediators neuroprotectin D1 and elovanoids in the retina during early pathogenesis in transgenic Alzheimer's disease 5xFAD mouse. These changes correlate with photoreceptor cell functional impairments preceding their loss. Amyloid beta (Aβ) peptide accumulates in drusen in AMD. Thus, injecting oligomeric Aβ in wild-type mice behind the retina leads to photoreceptor cell degeneration and transcriptional disruptions including upregulation of a senescence program and of senescence-associated secretory phenotype (SASP). Similar changes take place in human retinal pigment epithelium cells in culture. Novel lipid mediators, the elovanoids, restore Aβ-peptide-induced gene expression changes and SASP secretome and, in turn, protect these cells. This study opens avenues of potential therapeutic exploration of elovanoids for AMD.

Author contributions: K.V.D. and N.G.B. designed research; K.V.D., M.-A.I.K., B.J., W.C.G., R.N., R.Y., and N.A.P. performed research; K.V.D. and M.-A.I.K. performed OCT; M.-A.I.K. performed subretinal injection and ERG analysis; R.N., R.Y., and N.A.P. synthesized and purified the elovanoids; and K.V.D. and N.G.B. wrote the paper.

The authors declare no competing interest.

This article is a PNAS Direct Submission.

Data deposition: The data reported in this paper have been deposited in Dryad (DOI: 10.5061/dryad.59zw3r233).

[1]To whom correspondence may be addressed. Email: nbazan@lsuhsc.edu.

This article contains supporting information online at www.pnas.org/lookup/suppl/doi:10.1073/pnas.1912959116/-/DCSupplemental.

First published November 11, 2019.

senescence-associated secretory phenotype (SASP), to in turn, protect the RPE and sustain PRC integrity.

Results

5xFAD Mouse Retina and RPE Reveal Deficits in the Pathways Leading to NPD1 and ELVs Biosynthesis. When cleaved by PLA2 and PLA1, acyl chains of a phosphatidylcholine with DHA (at sn2) and VLC-PUFAs,n-3 (at sn1) lead to the synthesis of NPD1 and ELVs, respectively (10). To ascertain the availability of these PCs in the 5xFAD retinas and RPE, heat map analyses were performed. Two PC clusters emerged from these analyses: short chain (<48C) and saturated (<6 double bonds; group 1), and a less abundant cluster (group 2), when comparing the 5xFAD vs. WT (Fig. 1*A*). This means that 5xFAD retina has relatively less PC-containing VLC-PUFAs. However, principal component analysis did not reveal any sensible difference, since all discriminable makers for 5xFAD and WT mouse were short chain-containing PCs (Fig. 1 *B* and *C*). Hence, we performed a random forest classification with the criteria that the higher time used for the phosphatidylcholines, the more PC contribution to the variation of 5xFAD to WT would be highlighted. As a result, we found a dense distribution of high-time-used PCs in the VLC-PUFA-containing PC area (Fig. 1*D*), which supported the heat map analysis observation. Therefore, PCs were presented in 3 groups: DHA- and VLC-PUFA-containing PCs, DHA-containing PCs, and AA-containing PCs. Structures and *m*/*z* of PCs are depicted (*SI Appendix*, Fig. S2). The 5xFAD depicted decreases of both DHA- and VLC-PUFA-containing PCs, including PC54:12, PC56:12, and PC58:12 (Fig. 1*E*), and DHA-containing PCs, including PC36:8, PC38:8, and PC44:12 (Fig. 1*F*). In contrast, PCs containing AA, including PC36:4, PC38:4, and PC36:5, were increased in the 5xFAD retina (Fig. 1*G*), suggesting that the balance of n-6/n-3 (AA, DHA, and VLC-PUFA) was altered. Next, we

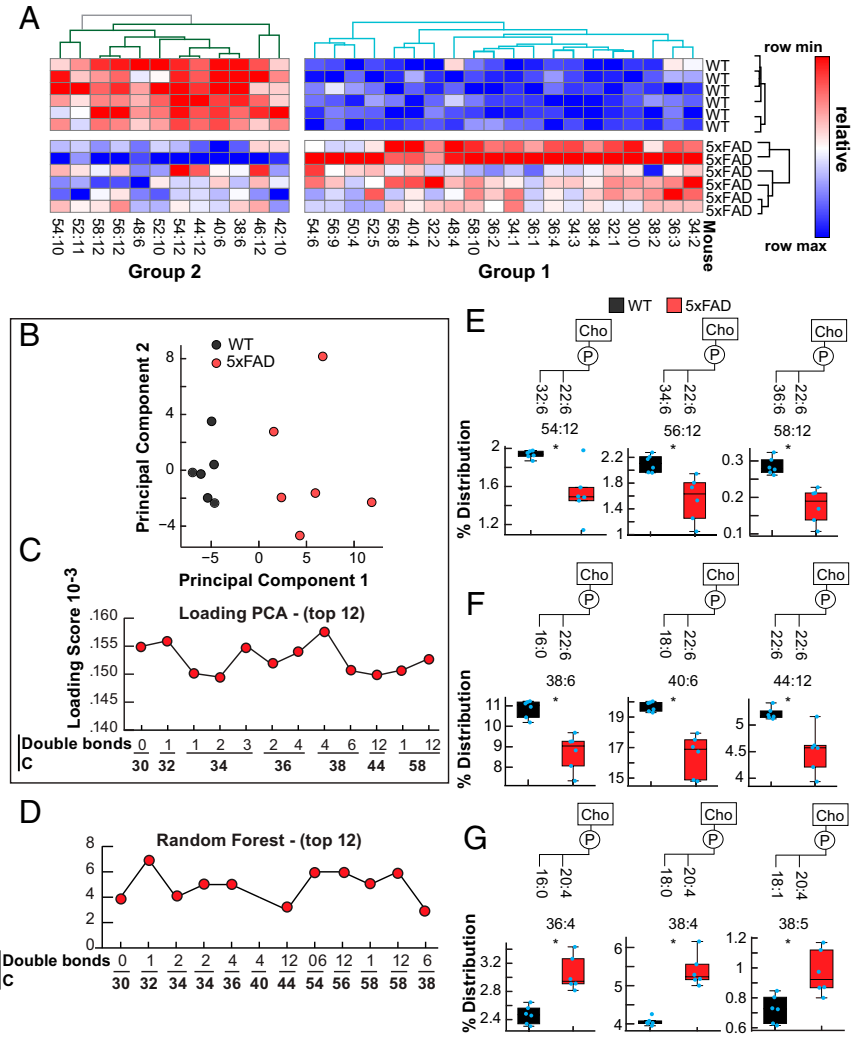

Fig. 1. Deficiency of VLC-PUFAs in phosphatidylcholine molecular species in the retina of the 5xFAD. (*A*) PCs heat map analysis of 6-mo-old 5xFAD ($n = 6$) and wild-type ($n = 6$). Two main clusters of PCs evolved with distinct features. Group 1 depicts abundant PCs in 5xFAD, whereas group 2 shows PCs prevalent in WT, with most PCs containing VLC-PUFAs. (*B*) Principal component analysis for PCs illustrates 2 populations (WT-black and 5xFAD-red) scatter across the principal component 1. Thus, the loading score for the principal component 1 is essential to identify distinct PCs for the difference between WT and 5xFAD. (*C*) The loading score (absolute values) of PCs to the principal component 1. The higher loading score, the more contribution of the PCs into principal component to distinguish WT and 5xFAD (*SI Appendix*, Fig. S1*A*). Ten short-chain PUFAs (<48C) contained in PCs are found in the top 12 most loading score PCs (*C*), while the VLC-PUFAs contained in PCs contribute 2 (58:1 and 58:12). (*D*) The time used in random forest classification for PCs of WT and 5xFAD. The higher time used, the more valuable of the PCs in WT and 5xFAD difference (*SI Appendix*, Fig. S1*B*). VLC-PUFAs contained PCs contribute 7 of 12 top times used in this classification (*D*). (*E*–*G*) Box plot for VLC-PUFAs (*E*), DHA (*F*), and AA (*G*) containing PCs. The WT has more VLC-PUFAs and DHA containing PCs, while the 5xFAD has more AA-contained PCs. (*$P < 0.05$, Student *t* test).

observed that DHA and VLC-PUFA contained in PCs were deficient in 5xFAD retina (Fig. 1 *A*–*G*), unlike in RPE (Fig. 2 *A*–*D*). The PC38:6 content was higher in the RPE of 5xFAD (contrast to the retina; Fig. 2*E*), and the PC40:6 was similar in 5xFAD and WT (Fig. 2*E*). PC44:12, however, was lower in the 5xFAD RPE, as in the retina. Furthermore, the relative abundance of PCs differs in retina and RPE. In retina, VLC-PUFA containing PCs amounted to 3% of total PC, while these PCs were less than 0.3% in the RPE. Similarly, PC44:12 was 5% in the retina and less than 0.5% in the RPE. Thus, PCs containing DHA and VLC-PUFA are more abundant in PRCs than RPE. Despite the small contribution of these PCs in RPE, our results clearly unveiled a deficiency of VLC-PUFA-containing PCs in the 5xFAD RPE.

ELVs are generated from VLC-PUFAs stored in PC54:12 and PC56:12, present in limited amounts in the 5xFAD retina and RPE (Figs. 1 and 2). We found that the free pool size of 32:6n3 and 34:6n3 are increased, reflecting release from the sn-1 position of the PC54:12 and PC56:12, respectively. We next explore the

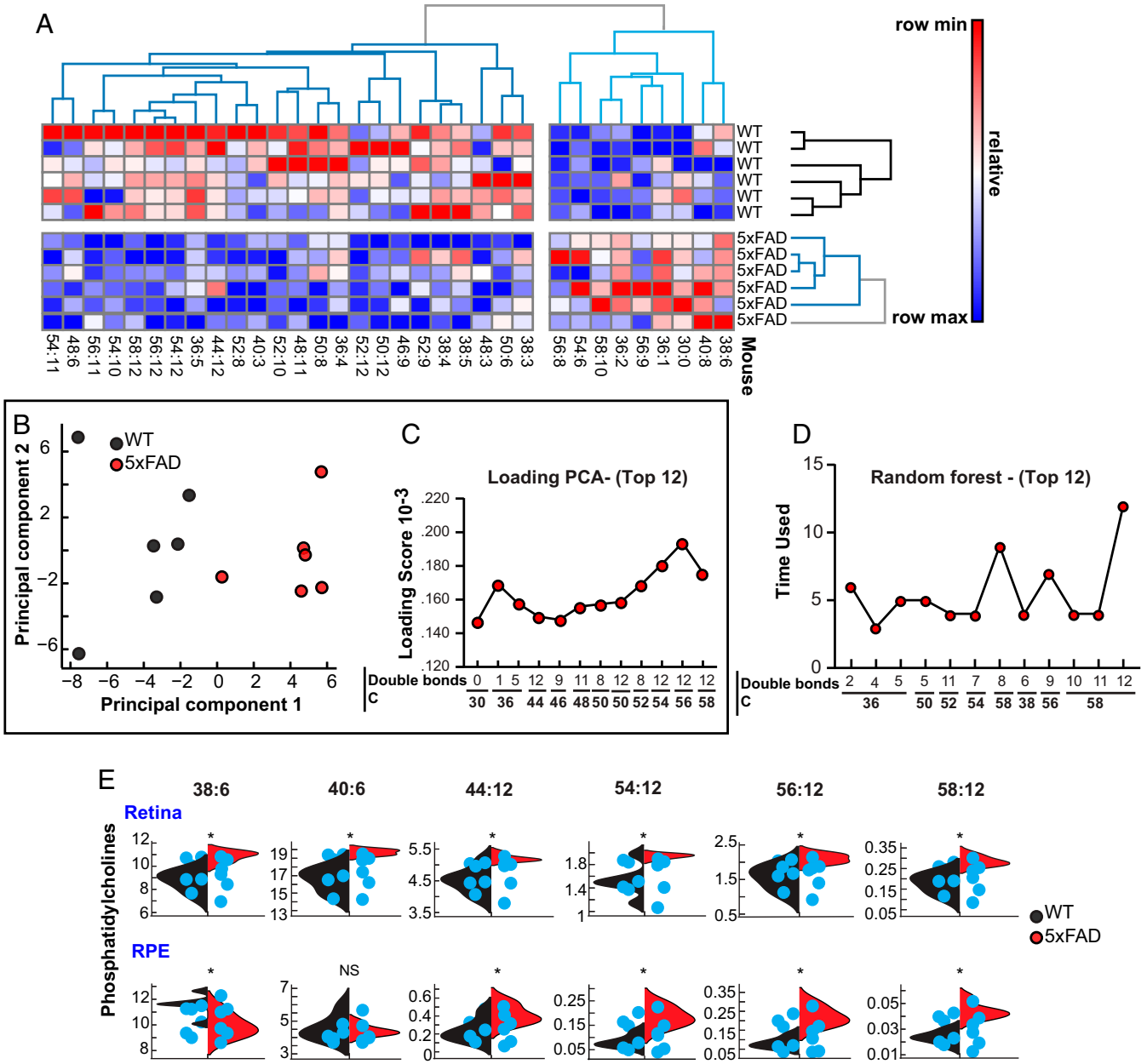

Fig. 2. Deficiency of VLC-PUFAs in phosphatidylcholine molecular species of the RPE of the 5xFAD. (*A*) Heat map analysis for PCs of 6-mo-old 5xFAD ($n = 6$) and WT ($n = 6$). VLC-PUFAs contained PCs are less abundant in 5xFAD. (*B*) Principal component analysis for PCs in RPE of 5xFAD and WT. There are 2 populations scatter across the principal component 1. However, it is not as clear as in the distribution in the retina (Fig. 1). For this reason, the loading score for principal component 1 is essential to identify the distinct PCs for the difference between WT and 5xFAD. (*C*) The loading score (absolute values) of PCs to principal component 1. The higher loading score, the more contribution of PCs into principal component 1 to distinguish WT and 5xFAD (*SI Appendix*, Fig. S1*C*). Six short-chain PUFAs (<48C) contained PCs found in the top 12 most loading score PCs (*C*), while the VLC-PUFAs contained PCs contributes 6 (50:8, 50:12, 52:8, 54:12, 56:12, and 58:12). (*D*) The time used in random forest classification for PCs of WT and 5xFAD. The higher time used, the more valuable of the PCs in WT and 5xFAD difference (*SI Appendix*, Fig. S1*D*). VLC-PUFAs contained PCs contribute 9 of 12 top time used in this classification (*D*). (*E*) Violin plot for percentage of PC38:6, PC40:6, and PC44:12 in the WT and 5xFAD retina (*Upper*) and eyecup (RPE, *Lower*). Surprisingly, the eyecup PCs show that 5xFAD has more PC38:6, less PC44:12, and equal PC40:6 to WT. NS, nonsignificant; *$P < 0.05$, Student *t* test.

subsequent, lipoxygenase-catalyzed enzymatic epoxidation to form the epoxide intermediate, followed by the hydrolase-catalyzed enzymatic hydrolysis, resulting in synthesis of di-hydroxylated ELV-N32 or ELV-N34 with the Z,E,E triene moiety (Fig. 3*A*). Thus, the expression of 15-lipoxygenase-1 in 5xFAD RPE is less than in WT, whereas in the retina, there are no differences between the 2 genotypes (Fig. 3 *C* and *D*), in agreement with NPD1 abundance that is lower in 5xFAD RPE and unchanged in the retina (Fig. 3*B*). In contrast, ELOVL4, an enzyme that elongates EPA or DHA, is only expressed in PRC and is lower in 5xFAD, correlating with the smaller pool size of 32:6n3 and 34:6n3, as well as of the monohydroxy stable derivatives of ELVs hydroperoxide precursors (Fig. 3 *B–D*). Therefore, lipids, as well as the expression of 2 key enzymes involved in the ELVs and NPD1 pathways, are markedly depressed in retina and RPE in early ages of retinal pathology development in the 5xFAD.

Early Abnormal Retina Function Preceding PRC Loss in 5xFAD. The b-wave ERG analysis of 6-mo-old 5xFAD mice discloses a loss of visual sensitivity (Fig. 4*A*). However, retinal ultrastructure, the RPE cell/Bruch's membrane interface, the outer segment basal region of disk synthesis, the integrity of the outer limiting membrane, elongate inner segment mitochondria (no fission profiles), and PRC tip release and phagocytosis by the RPE (Fig. 4*B*) demonstrated the lack of abnormalities. Furthermore, histology did not show PRC loss of 5xFAD (Fig. 4*C*). In contrast, immunofluorescence microscopy showed that in 5xFAD, the Aβ is mainly accumulated in the retina under the RPE, as in AMD phenotype of drusen (Fig. 4*D*).

ELVs Protect RPE and PRC against OAβ-Induced Toxicity. Because of the early deficits in the prohomeostatic pathways leading to ELVs synthesis in 5xFAD retina, and the ensuing retinal degeneration, we next asked whether ELVs would protect against the effect of

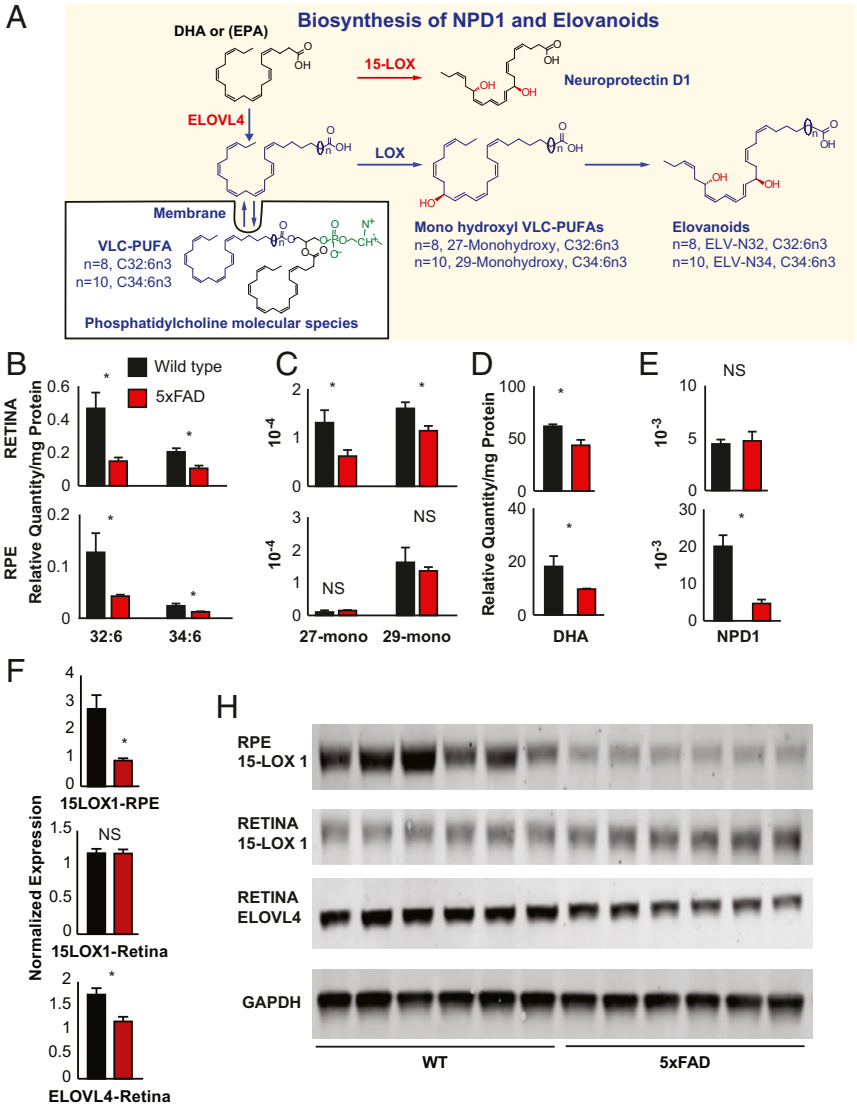

Fig. 3. Deficiencies in precursors and intermediates of lipid mediator pathways and of ELOVL-4 during the early development of retina pathology in the 5xFAD. (*A*) Biosynthetic pathways of NPD1 and of 32:6n3 and 34:6n3 ELVs from PC 54:12 and PC56:12. (*B*) Free 32:6n3 and 34:6n3. (*C*) 27-monohydroxy 32:6n3 and 29-monohydroxy 34:6n3, stable derivatives of the hydroperoxyl-precursors of ELV-N32 and ELV-N34, respectively. (*D*) Free DHA. (*E*) NPD1. In *B–E*, retina (*Top*) and RPE (*Bottom*) ($n = 6$/group). (*F* and *G*) 115-LOX-1 and ELOVL4 Western blots and quantification in RPE and retina ($n = 6$/group). In RPE, 15-lipoxygenase-1 in 5xFAD is less than WT. In retina, there is no difference between 2 groups. This is in agreement with lower NPD1 pool size in 5xFAD, but no change in retina (*E*). ELOVL4 is only expressed in retina and is lower in 5xFAD. As a consequence, there was less free 32:6n3 and 34:6n3, as well as less abundant monohydroxy stable precursor derivatives. NS, nonsignificant; $^*P < 0.05$, Student *t* test.

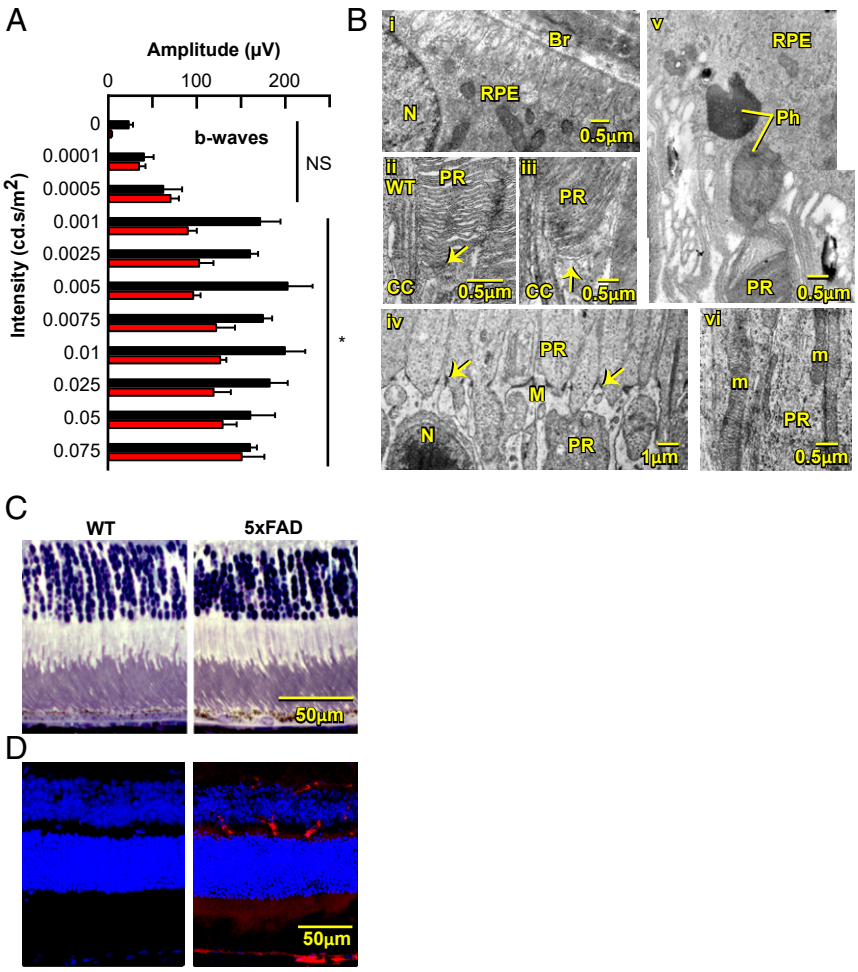

Fig. 4. Morphology and function of the 5xFAD retina. (*A*) V log I plot showing maximum ERG b-wave amplitudes for light flashes from 0 to 0.075 cd·s/m^2. 5xFAD achieved maximum amplitude of about 100 μV, approximately half that recorded for WT (n = 6/group). (*B*) Electron microscopy of 6-mo-old 5xFAD retinas illustrating similarities to WT. (*B*, *i*) Basal side of a 5xFAD RPE cell showing membrane infoldings along Bruch's membrane (Br). (*B*, *ii*) Disk synthesis region (arrow) at basal portion of a rod outer segment showing newly formed disks from the connecting cilium (CC) membrane (WT). (*B*, *iii*) Similar region in a 5xFAD displaying new disk formation (arrow). (*B*, *iv*) The outer limiting membrane (arrow) at the scleral edge of the cell body layer (N, photoreceptor nucleus) in the 5xFAD. The cytoplasm of Müller cells (M) appears lighter than that of PRC. (*B*, *v*) The interface between a 5xFAD RPE cell and a rod PRC tip (PR). Two phagosomes (Ph) within the RPE cytoplasm; the *Lower* Ph is held within the RPE apical processes, while the *Upper*, darker Ph is older and just entering the RPE cell body, illustrating normal phagocytic function. (*B*, *vi*) Inner segment mitochondria (M) of 5xFAD retain the typical very elongate PRC. (*C*) Five-month-old WT and 5xFAD retinal sections illustrating normal PRC profiles within the 5xFAD retina. (*D*) Fluorescent staining of the retina from WT and 5xFAD. The blue (DAPI) is the nuclei and red Aβ in the RPE layer at 6 mo old in 5xFAD. *P < 0.05, Student t test.

OAβ, a most cytotoxic Aβ peptide (18). Six-month-old WT mice subretinally injected with OAβ demonstrated PRC degeneration (Fig. 5 *A* and C). Fundus (left side) and corresponding optical coherence tomography (OCT; right side) images are depicted. The PRC layer underwent cell loss from 105 μm thickness for the noninjected retina to 35 μm for the OAβ-injected retina. Noninjected, PBS-injected, and ELV-N32, ELV-N34-injected mice did not yield PRC degeneration (Fig. 5 *C* and *D*). The ZO-1 staining of flat-mounted RPE revealed that OAβ disrupted tight junctions and triggered cell damage. We coinjected ELV-N32 or ELV-N34 with OAβ, followed by topical application of the ELVs over the course of 7 d (Fig. 5*A*), resulting in restoration of RPE morphology (Fig. 5*B*) and protection of PRC (Fig. 5 *C* and *D*). The mice injected with PBS or ELVs alone showed a small reduction of ONL, likely because of mechanical stress after subretinal injection (Fig. 5 *C* and *D*). These results demonstrate that ELVs preserve the integrity of PRC, which denotes the ability of these lipid mediators to counteract cellular injury sustained by OAβ toxicity.

ELVs Counteract OAβ-Induced Senescence, Autophagy, AMD, and ECM Remodeling Gene Expression Disruptions in RPE and Apoptotic Gene Expression in Retina. To search for the mechanism or mechanisms involved in ELVs protection against OAβ-mediated damage, isolated RPE and retina were subjected to quantitative PCR. We selected to survey genes that were involved in senescence (19, 20), autophagy (21), AMD (22, 23), and ECM remodeling (24) on day 3 postinjection in the RPE (Fig. 5 *E*–*G*). In addition, we explored cell death-related genes that encode the proteins Bax, Bad, Casp3, Dapk1, and Fas in the retina (Fig. 5*I*). The OAβ-mediated upregulation of senescence, autophagy, AMD, and some ECM remodeling gene expression was counteracted by ELVs (Fig. 5). Certain matrix metalloproteinases (1b, 10, 14, 7) were not affected by OAβ. In addition, in the RPE, the protein abundance of the key senescence p16^{INK4a} (Fig. 5*H*) correlates with those on its gene expression (Fig. 5*E*).

ELVs Protect Human RPE Cells from OAβ-Induced Senescence and Other Gene Transcription Disruptions. Because 5xFAD mice display RPE tight junction disruptions on Aβ accumulation (16), we

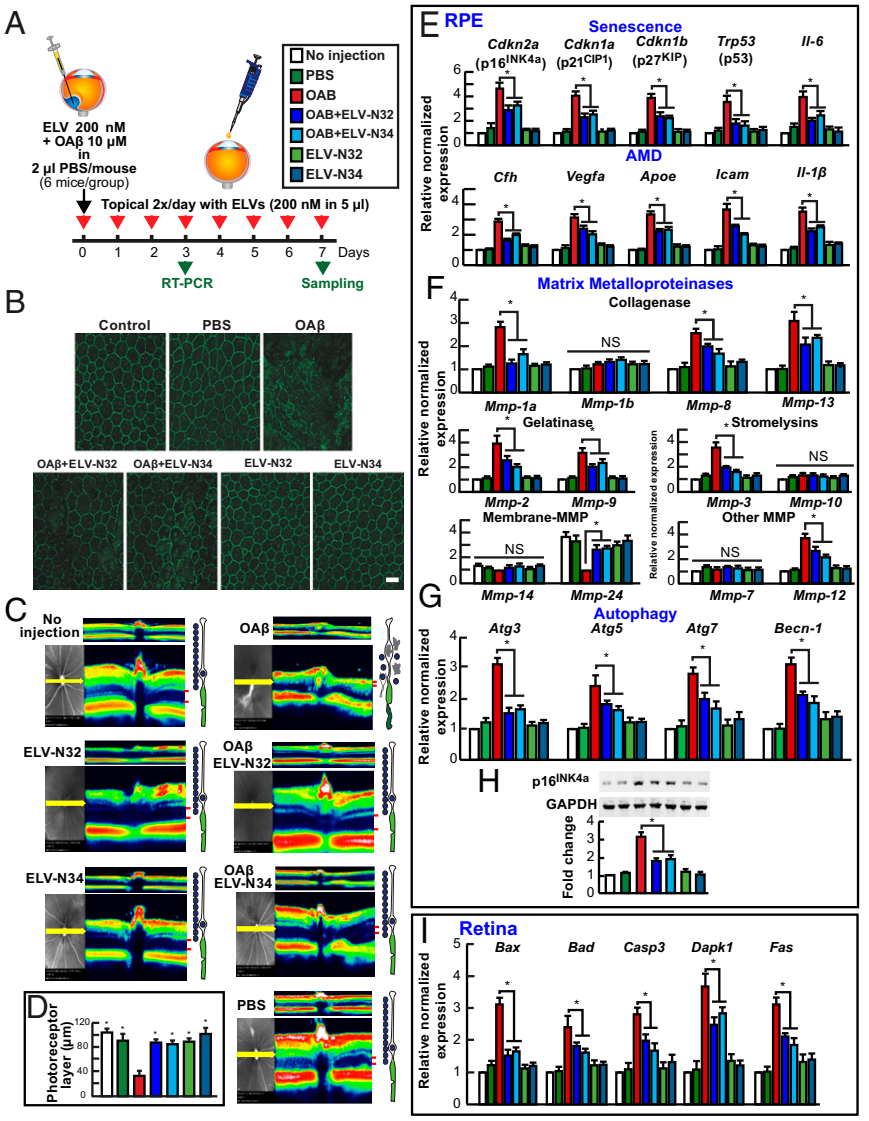

Fig. 5. ELVs restore RPE morphology and reduce gene expression after subretinal injection of OAβ in WT mice. (*A*) In vivo experimental design: 6-mo-old C57BL/6J WT mice were divided into 7 groups (n = 12/group): noninjected, PBS, OAβ only, OAβ+ELV-N32, OAβ+ELV-N34, ELV-N32 only, and ELV-N34 only. On day 3, mRNA were isolated for real-time PCR. On day 7, mice were subjected to OCT and then eyes enucleated and processed for whole-mount RPE staining and Western blots. (*B*) Whole flat mount of RPE with tight junction marker, Zonula occludens-1 (ZO-1) antibody. OAβ disrupted RPE morphology. (*C*) OAβ effects on retina and RPE by OCT. (*D*) Thickness of PRC layer was thinner in OAβ-injected group. (*E*) RPE gene expression after OAβ (1 to 42) injection and treatment with ELVs. (*E–G*) Gene expression in the same functional group were plotted. Senescence- and AMD-related genes (*E*), and collagenases, gelatinase, stromelysins, and other matrix metalloproteinases (MMP) (*F*) and autophagy (*G*). (*H*) p16^{INK4a}, a key marker for senescence, Western blots of RPE. (*I*) Retina apoptosis gene expression after OAβ (1 to 42) injection and treatment with ELVs. *$P < 0.05$, Student t test.

used a primary human RPE cell in culture challenged with OAβ to assess damage and to evaluate possible ELV-N32 or ELV-N34 protection (Fig. 6*A*). After 7 d incubation, OAβ altered RPE cell morphology and activated SASP, as revealed by the SA-β-Gal staining (Fig. 6 *B* and *C*), as well as enhanced the expression of a set of senescence genes (Fig. 5*E*), AMD, matrix metalloproteinases, and autophagy-related genes (Fig. 6*D*). A point of interest is that some matrix metalloproteinases were affected, but not all were expressed in RPE cells. In other cells, SASP is primarily proinflammatory and has been shown to comprise chemokines, metalloproteinases, proteases, cytokines (e.g., TNF-α, IL-6, and IL-8), and insulin-like growth factor binding proteins. The senescence genes studied are p16^{INK4a} (Cdkn2a), p21^{CIP1}(Cdkn1A), p27^{KIP} (Cdkn1B), p53 (Tp53 or TRP53), IL6, and MMP1. ELV-N32 and ELV-N34 reverted these effects (Fig. 6 *B–D*).

Discussion

AMD and AD display accumulation of Aβ in the retina and brain, respectively. Aβ-based antibody, as well as anti-inflammatory therapies for AD, have been largely unsuccessful; therefore, there is a need to understand mechanisms and identify specific agents that limit Aβ neurotoxicity (25–28). RPE sustains PRC integrity, and its dysfunction sets in motion PRC death in retinal degenerative diseases, including AMD. Here we show that OAβ drives RPE and PRC pathology, both in vivo in a rodent and in primary human RPE cell culture. Early in the pathogenesis of 5xFAD PRC degeneration, we report deficits in precursors and pathways for NPD1 and ELVs biosynthesis. These deficits precede ECM and histology signs of PRC damage, while ERG already displays impairments. These findings uncover potential prodromal alterations of key prohomeostatic lipid signaling during onset and early disease progression. Aside from

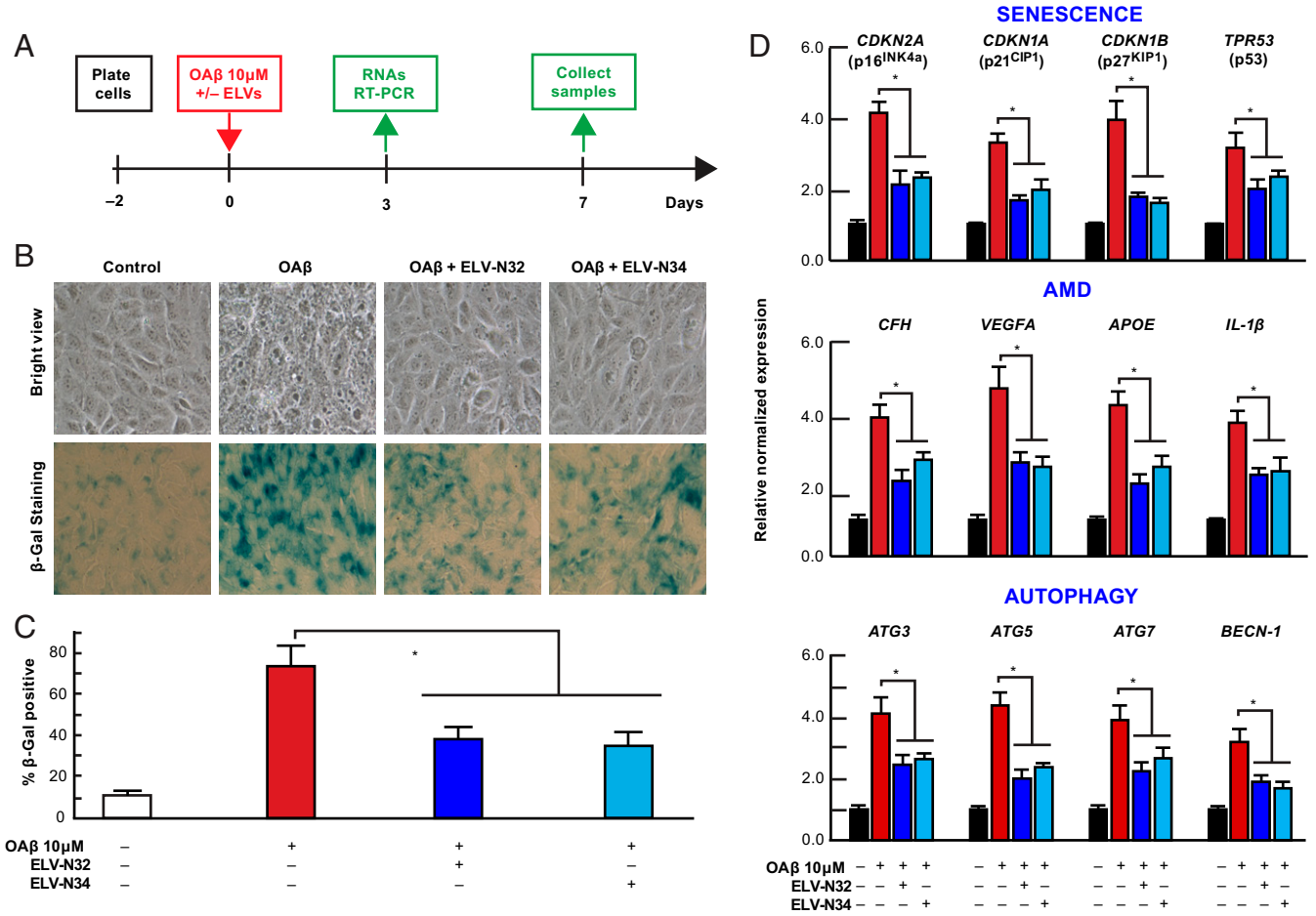

Fig. 6. OA-β-mediated activation of senescence-associated secretory phenotype (β-galactosidase, SA-β-Gal) and of gene expression in human RPE cells in primary culture are counteracted by ELVs. (*A*) In vitro experimental design: primary human RPE cells were treated with 10 μM OAβ ±ELVs. After 3 d, RNA was isolated and quantitative PCR analyzed. After 7 d, cells were subjected to β-galactosidase staining. (*B*) Live cell images under bright field microscopy after 7 d. (*C*) β-Gal staining ±ELVs. Quantitation of percentage for the β-Gal-positive cells. ELVs decreased positive senescent cells. (*D*) Gene transcription of senescence, AMD-related, and autophagy genes after OAβ (1 to 42) exposure ±ELVs. $*P < 0.05$, Student *t* test.

being used as biomarkers, they can also be explored as therapeutic targets for AMD.

There is not clear evidence in genetic animal models that blocking Aβ formation results in reduced AMD pathology. However, there are studies aiming to inhibit Aβ in the eye experimentally to protect PRC. For example, Liu et al. (29) showed that 10 mo of Aβ vaccination inhibits retinal deposits, but causes retinal amyloid angiopathy characterized by microglial infiltration and astrogliosis in AD-transgenic mice. A drawback to this is the fact that active immunization can cause severe adverse effects.

It is not clear how many patients with AD develop AMD, nor vice versa. However, there is a correlation between AD and eye diseases other than AMD that includes glaucoma and susceptibility to diabetic retinopathy (30). Evolving key signaling disease mechanisms, include CFH, APOE (31–33), and the matrix metalloproteinase pathway (34). Our data show that subretinal OAβ injection in mice triggers RPE cell damage and PRC loss after 7 d. To test the soundness of the Aβ deleterious effects on the RPE, we used human RPE cells in primary cultures and showed that it sets in motion similar damage as in the in vivo rodent. Moreover, both in the rodent model in vivo and in human cells in vitro, the changes in gene expression profiles were similar. Aβ synthesis takes place in the RPE (35–38) and accumulates in drusen; it is becoming evident that amyloid precursor protein processing dysfunctions lead as well to accumulation of the peptide within the retina also adjacent to ganglion cells, and to the inner nuclear layer (39–41), and its synthesis, abundance, secretion, and aggregation increases in an age-dependent fashion (39). Our subretinal injection of Aβ here recapitulates some conditions associated with pathology of AMD particularly targeting the RPE.

The finding that OAβ-induced RPE and PRC death in wild-type mice in vivo was counteracted by ELVs uncovers additional bioactivity of these specific downstream mediators from omega-3 fatty acids. Mechanistically, neuroinflammatory disruptions are involved in early stages of AMD pathology, and several studies have used dietary supplementation with omega-3 fatty acids (42–46), which have not yielded clear benefits, likely because the supply of these critical fatty acids to the PRC and synapses involves complex steps that include gut, liver, blood stream transport, cellular uptake, and so on (47, 48). A rational therapeutic approach for AMD would be to use mediators from omega-3 fatty acids that have neuroprotective bioactivity.

The present study identifies ELVs 32 and 34 as downregulatory mediators of OAβ-evoked senescence, as shown by SASP and the expression of senescence-related genes in RPE. Under these conditions, the up-regulated expression of autophagy- and AMD-related genes, including human complement factor (49) and extracellular matrix genes, were beneficially targeted by ELVs as well. Thus, the similarities on the OAβ elicited effects in RPE cells in culture and in RPE and PRC in vivo, including the ELV-targeted

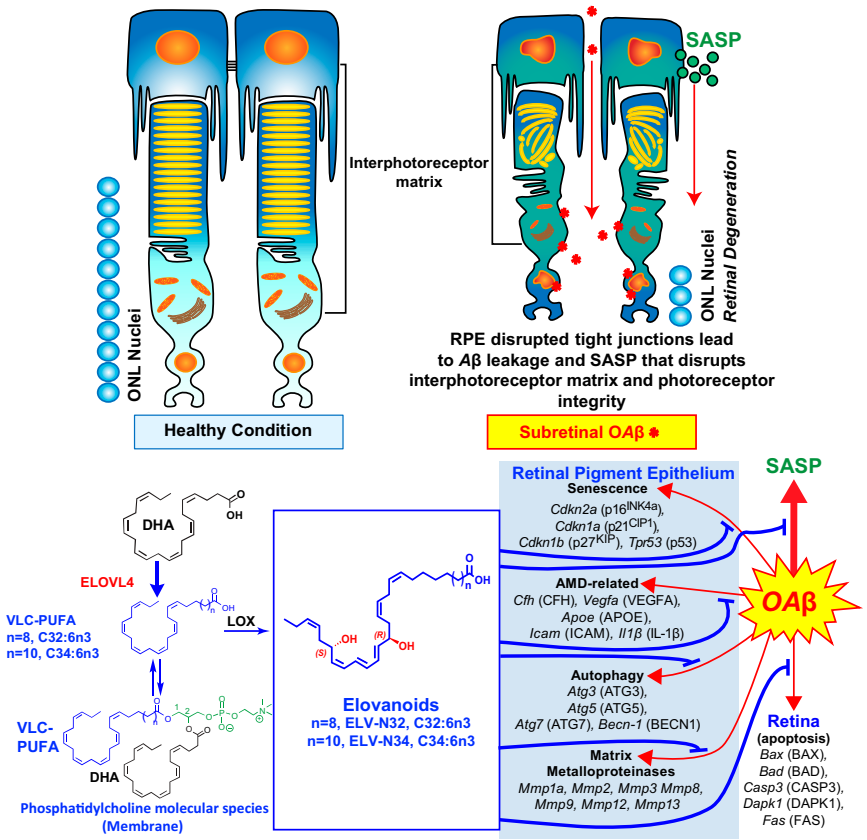

Fig. 7. Summary of ELVs effects on OAβ-induced RPE and PRC damage. (*A*) OAβ induces a senescence program and disrupts RPE tight junctions. OAβ penetrates the retina, causing PRC cell death in our in vivo WT mice study as reflected in less outer nuclear layer (ONL) nuclei (Fig. 5). OAβ activates the senescence-associated secretome (SASP) that contributes to perturbing the interphotoreceptor matrix (IPM), triggering inflammaging in PRC and also likely in Mueller glia, which limits the IPM. Therefore, senescence paracrine expression takes place. ELVs restore RPE morphology and PRC integrity (Fig. 5). (*B*) OAβ induces expression of senescence, autophagy, matrix metalloproteinases, and AMD-related genes in the RPE and apoptosis genes in retina in addition to $p16^{INK4a}$ protein abundance (Fig. 5*H*). ELVs down-regulated the OAβ-gene inductions and $p16^{INK4a}$ protein abundance. Pathways for the ELV synthesis are outlined.

protection, suggest relevance to the human retina. Surprisingly, we observed that OAβ injection caused apoptosis-related cell death signaling in photoreceptor cells, not senescence. However, it is important to note that ELVs prevented both OAβ-induced senescence in RPE and OAβ-induced PRC apoptosis.

In conclusion, we uncovered early deficits of prohomeostatic pathways before PRC death in the 5xFAD mice, highlighted by decreased abundance of PC molecular species in RPE (particularly those containing VLC-PUFAs) and in retina (those containing DHA and VLC-PUFAs). Also, the pool size of free VLC-PUFAs and stable derivatives of precursors 27- and 29-monohydoxy and of ELV-N32 and ELV-N34, respectively, were found to be depleted. Moreover, the retina displays deficiencies in key enzymes of the pathways for the synthesis of prohomeostatic/neuroprotective NPD1 and ELVs without overt PRC damage or loss, but shows functional impairments. ELVs counteracted the cytotoxicity of OAβ subretinally administered in WT mice leading to RPE tight junction disruptions followed by PRC cell death. Our data show that OAβ activates a senescence program reflected by enhanced gene expression of *Cdkn2a*, *Mmp1a*, *Trp53*, *Cdkn1a*, *Cdkn1b*, Il-6, and SASP secretome, followed by RPE and PRC demise (Fig. 7), and that ELV-N32 and ELV-N34 blunt these events and elicit protection to both cells. $P16^{INK4a}$ protein abundance is also targeted. The RPE cell is terminally differentiated and originated from the neuroepithelium. In this connection, senescent neurons in aged mice and models of AD (50) and astrocytes (51, 52) also express senescence and develop secretory SASP that fuel neuroinflammation in nearby cells (53–55). This is likely the case in our present study, where neighbor cells may be targeted by SASP neurotoxic actions, inducing photoreceptor paracrine senescence. Therefore, SASP from RPE cells may be autocrine and paracrine, altering the homeostasis of the interphotoreceptor matrix microenvironment (Fig. 7) as a consequence, and creating an inflammatory milieu that contributes to loss of function associated with aging (56), age-related pathologies (56) AD, and likely AMD. Furthermore, ELVs restore expression of ECM remodeling matrix metalloproteinases altered by OAβ treatment, pointing to an additional disturbance in the interphotoreceptor matrix. The inflammation set in motion may be a low-grade, sterile, chronic proinflammatory condition similar to inflammaging that is also linked to senescence of the immune system (56, 57). In addition, ELVs counteracted OAβ-induced expression of genes engaged in AMD and autophagy. It remains to be defined whether the ELVs targeted events on gene transcription (Fig. 7) to inform novel unifying regulatory mechanisms to sustain health span during aging and neurodegenerative diseases (56, 58). Several forms of retinal degenerative diseases, including retinitis pigmentosa and other inherited retinal degenerations, may underlie these mechanisms, and ELVs might halt the onset or slow down disease progression. Although further research is needed, our results, overall, show the potential of ELVs as a possible therapeutic avenue of exploration for AMD.

Materials and Methods

Materials and methods used in this study are described in detail in *SI Appendix, SI Materials and Methods*. This information includes animals, lipid

extraction, and LC-MS/MS-based lipidomic analysis, primary human RPE culture, Aβ (1 to 42) oligomerization, senescence-associated secretory phenotype by β-Gal staining, protein extraction and Western blot analysis, RNA isolation and quantitative PCR analysis, immunofluorescence and confocal microscopy, and statistics.

Data Availability. The data reported in this paper have been deposited in Dryad (DOI: 10.5061/dryad.59zw3r233) (59).

ACKNOWLEDGMENTS. This study was supported by the National Institutes of Health/National Eye Institute grant R01 EY005121 and the Eye Ear Nose & Throat Foundation.

1. N. G. Bazan, Cell survival matters: Docosahexaenoic acid signaling, neuroprotection and photoreceptors. *Trends Neurosci.* **29**, 263–271 (2006).
2. W. J. Lukiw *et al*., A role for docosahexaenoic acid-derived neuroprotectin D1 in neural cell survival and Alzheimer disease. *J. Clin. Invest.* **115**, 2774–2783 (2005).
3. L. V. Johnson *et al*., The Alzheimer's A beta -peptide is deposited at sites of complement activation in pathologic deposits associated with aging and age-related macular degeneration. *Proc. Natl. Acad. Sci. U.S.A.* **99**, 11830–11835 (2002).
4. D. H. Anderson *et al*., Characterization of beta amyloid assemblies in drusen: The deposits associated with aging and age-related macular degeneration. *Exp. Eye Res.* **78**, 243–256 (2004).
5. M.-P. Agbaga *et al*., Role of Stargardt-3 macular dystrophy protein (ELOVL4) in the biosynthesis of very long chain fatty acids. *Proc. Natl. Acad. Sci. U.S.A.* **105**, 12843–12848 (2008).
6. R. Harkewicz *et al*., Essential role of ELOVL4 protein in very long chain fatty acid synthesis and retinal function. *J. Biol. Chem.* **287**, 11469–11480 (2012).
7. M. I. Aveldaño, Phospholipid species containing long and very long polyenoic fatty acids remain with rhodopsin after hexane extraction of photoreceptor membranes. *Biochemistry* **27**, 1229–1239 (1988).
8. M. A. Aldahmesh *et al*., Recessive mutations in ELOVL4 cause ichthyosis, intellectual disability, and spastic quadriplegia. *Am. J. Hum. Genet.* **89**, 745–750 (2011).
9. B. Jun *et al*., Elovanoids are novel cell-specific lipid mediators necessary for neuroprotective signaling for photoreceptor cell integrity. *Sci. Rep.* **7**, 5279 (2017).
10. N. G. Bazan, Docosanoids and elovanoids from omega-3 fatty acids are pro-homeostatic modulators of inflammatory responses, cell damage and neuroprotection. *Mol. Aspects Med.* **64**, 18–33 (2018).
11. S. Bhattacharjee *et al*., Elovanoids are a novel class of homeostatic lipid mediators that protect neural cell integrity upon injury. *Sci. Adv.* **3**, e1700735 (2017).
12. T. Dentchev, A. H. Milam, V. M.-Y. Lee, J. Q. Trojanowski, J. L. Dunaief, Amyloid-beta is found in drusen from some age-related macular degeneration retinas, but not in drusen from normal retinas. *Mol. Vis.* **9**, 184–190 (2003).
13. M. T. Heneka *et al*., Neuroinflammation in Alzheimer's disease. *Lancet Neurol.* **14**, 388–405 (2015).
14. T. Prasad *et al*., Amyloid β peptides overexpression in retinal pigment epithelial cells via AAV-mediated gene transfer mimics AMD-like pathology in mice. *Sci. Rep.* **7**, 3222 (2017).
15. K. H. Kurji *et al*., Microarray analysis identifies changes in inflammatory gene expression in response to amyloid-beta stimulation of cultured human retinal pigment epithelial cells. *Invest. Ophthalmol. Vis. Sci.* **51**, 1151–1163 (2010).
16. S. W. Park *et al*., Dry age-related macular degeneration like pathology in aged 5XFAD mice: Ultrastructure and microarray analysis. *Oncotarget* **8**, 40006–40018 (2017).
17. C. Criscuolo *et al*., The retina as a window to early dysfunctions of Alzheimer's disease following studies with a 5xFAD mouse model. *Neurobiol. Aging* **67**, 181–188 (2018).
18. B. A. Yankner, T. Lu, Amyloid beta-protein toxicity and the pathogenesis of Alzheimer disease. *J. Biol. Chem.* **284**, 4755–4759 (2009).
19. R. Salama, M. Sadaie, M. Hoare, M. Narita, Cellular senescence and its effector programs. *Genes Dev.* **28**, 99–114 (2014).
20. P. Zhang *et al*., Senolytic therapy alleviates Aβ-associated oligodendrocyte progenitor cell senescence and cognitive deficits in an Alzheimer's disease model. *Nat. Neurosci.* **22**, 719–728 (2019).
21. S. K. Mitter *et al*., Dysregulated autophagy in the RPE is associated with increased susceptibility to oxidative stress and AMD. *Autophagy* **10**, 1989–2005 (2014).
22. C. B. Toomey, L. V. Johnson, C. Bowes Rickman, Complement factor H in AMD: Bridging genetic associations and pathobiology. *Prog. Retin. Eye Res.* **62**, 38–57 (2018).
23. M. M. DeAngelis *et al*., Genetics of age-related macular degeneration (AMD). *Hum. Mol. Genet.* **26** (RS1), R45–R50 (2017).
24. B. Budiene *et al*., The association of matrix metalloproteinases polymorphisms and interleukins in advanced age-related macular degeneration. *Ophthalmic Genet.* **39**, 463–472 (2018).
25. F. Panza, M. Lozupone, G. Logroscino, B. P. Imbimbo, A critical appraisal of amyloid-β-targeting therapies for Alzheimer disease. *Nat. Rev. Neurol.* **15**, 73–88 (2019).
26. P. L. McGeer, E. G. McGeer, The amyloid cascade-inflammatory hypothesis of Alzheimer disease: Implications for therapy. *Acta Neuropathol.* **126**, 479–497 (2013).
27. A. C. Cuello, Early and late CNS inflammation in Alzheimer's disease: Two extremes of a continuum? *Trends Pharmacol. Sci.* **38**, 956–966 (2017).
28. A. Crane *et al*., Peripheral complement interactions with amyloid β peptide in Alzheimer's disease: 2. Relationship to amyloid β immunotherapy. *Alzheimers Dement.* **14**, 243–252 (2018).
29. B. Liu *et al*., Amyloid-peptide vaccinations reduce beta-amyloid plaques but exacerbate vascular deposition and inflammation in the retina of Alzheimer's transgenic mice. *Am. J. Pathol.* **175**, 2099–2110 (2009).
30. C. S. Lee *et al*., Associations between recent and established ophthalmic conditions and risk of Alzheimer's disease. *Alzheimers Dement.* **15**, 34–41 (2019).
31. L. Biscetti *et al*., Associations of Alzheimer's disease with macular degeneration. *Front. Biosci. (Elite Ed.)* **9**, 174–191 (2017).
32. M. A. Williams *et al*., Age-related macular degeneration-associated genes in Alzheimer disease. *Am. J. Geriatr. Psychiatry* **23**, 1290–1296 (2015).
33. S. Frost *et al*.; AIBL Research Group, Alzheimer's disease and the early signs of age-related macular degeneration. *Curr. Alzheimer Res.* **13**, 1259–1266 (2016).
34. A. A. Hussain, Y. Lee, J.-J. Zhang, P. T. Francis, J. Marshall, Disturbed matrix metalloproteinase pathway in both age-related macular degeneration and Alzheimer's disease. *J. Neurodegener. Dis.* **2017**, 4810232 (2017).
35. S. A. Lynn *et al*., The complexities underlying age-related macular degeneration: Could amyloid beta play an important role? *Neural Regen. Res.* **12**, 538–548 (2017).
36. J. A. Ratnayaka, L. C. Serpell, A. J. Lotery, Dementia of the eye: The role of amyloid beta in retinal degeneration. *Eye (Lond.)* **29**, 1013–1026 (2015).
37. T. Yoshida *et al*., The potential role of amyloid beta in the pathogenesis of age-related macular degeneration. *J. Clin. Invest.* **115**, 2793–2800 (2005).
38. J. Wang, K. Ohno-Matsui, I. Morita, Elevated amyloid β production in senescent retinal pigment epithelium, a possible mechanism of subretinal deposition of amyloid β in age-related macular degeneration. *Biochem. Biophys. Res. Commun.* **423**, 73–78 (2012).
39. J. Wang *et al*., Development and expression of amyloid-β peptide 42 in retinal ganglion cells in rats. *Anat. Rec. (Hoboken)* **294**, 1401–1405 (2011).
40. R. M. Dutescu *et al*., Amyloid precursor protein processing and retinal pathology in mouse models of Alzheimer's disease. *Graefes Arch. Clin. Exp. Ophthalmol.* **247**, 1213–1221 (2009).
41. J. Hoh Kam, E. Lenassi, G. Jeffery, Viewing ageing eyes: Diverse sites of amyloid beta accumulation in the ageing mouse retina and the up-regulation of macrophages. *PLoS One* **5**, e13127 (2010).
42. M. Fiala, G. Kooij, K. Wagner, B. Hammock, M. Pellegrini, Modulation of innate immunity of patients with Alzheimer's disease by omega-3 fatty acids. *FASEB J.* **31**, 3229–3239 (2017).
43. F. La Rosa *et al*., The gut-brain axis in Alzheimer's disease and omega-3. A critical overview of clinical trials. *Nutrients* **10**, E1267 (2018).
44. N. M. D'Cunha *et al*., Effect of long-term nutraceutical and dietary supplement use on cognition in the elderly: A 10-year systematic review of randomised controlled trials. *Br. J. Nutr.* **119**, 280–298 (2018).
45. M. Belkouch *et al*., The pleiotropic effects of omega-3 docosahexaenoic acid on the hallmarks of Alzheimer's disease. *J. Nutr. Biochem.* **38**, 1–11 (2016).
46. J. G. Devassy, S. Leng, M. Gabbs, M. Monirujjaman, H. M. Aukema, Omega-3 polyunsaturated fatty acids and oxylipins in neuroinflammation and management of Alzheimer disease. *Adv. Nutr.* **7**, 905–916 (2016).
47. N. G. Bazan, M. F. Molina, W. C. Gordon, Docosahexaenoic acid signalolipidomics in nutrition: Significance in aging, neuroinflammation, macular degeneration, Alzheimer's, and other neurodegenerative diseases. *Annu. Rev. Nutr.* **31**, 321–351 (2011).
48. D. S. Rice *et al*., Adiponectin receptor 1 conserves docosahexaenoic acid and promotes photoreceptor cell survival. *Nat. Commun.* **6**, 6228 (2015).
49. M. Landowski *et al*., Human complement factor H Y402H polymorphism causes an age-related macular degeneration phenotype and lipoprotein dysregulation in mice. *Proc. Natl. Acad. Sci. U.S.A.* **116**, 3703–3711 (2019).
50. N. Musi *et al*., Tau protein aggregation is associated with cellular senescence in the brain. *Aging Cell* **17**, e12840 (2018).
51. M. M. Das, C. N. Svendsen, Astrocytes show reduced support of motor neurons with aging that is accelerated in a rodent model of ALS. *Neurobiol. Aging* **36**, 1130–1139 (2015).
52. C. Turnquist *et al*., p53 isoforms regulate astrocyte-mediated neuroprotection and neurodegeneration. *Cell Death Differ.* **23**, 1515–1528 (2016).
53. S. H. Appel, W. Zhao, D. R. Beers, J. S. Henkel, The microglial-motoneuron dialogue in ALS. *Acta Myol.* **30**, 4–8 (2011).
54. O. Komine, K. Yamanaka, Neuroinflammation in motor neuron disease. *Nagoya J. Med. Sci.* **77**, 537–549 (2015).
55. V. V. Lunyak, A. Amaro-Ortiz, M. Gaur, Mesenchymal stem cells secretory responses: Senescence messaging secretome and immunomodulation perspective. *Front. Genet.* **8**, 220 (2017).
56. J. Campisi *et al*., From discoveries in ageing research to therapeutics for healthy ageing. *Nature* **571**, 183–192 (2019).
57. S. He, N. E. Sharpless, Senescence in health and disease. *Cell* **169**, 1000–1011 (2017).
58. D. J. Baker *et al*., Naturally occurring p16(Ink4a)-positive cells shorten healthy lifespan. *Nature* **530**, 184–189 (2016).
59. N. G. Bazan, *et al*., Elovanoids counteract oligomeric β-Amyloid-induced gene expression and protect photoreceptors. Dryad. https://datadryad.org/stash/dataset/doi:10.5061/dryad.59zw3r233. Deposited 25 September 2019.